Supporting Information

"Computational calorimetry: High-precision calculation of host-guest binding thermodynamics".
Niel M. Henriksen, Andrew T. Fenley, and Michael K. Gilson*
*Contact: mgilson@ucsd.edu

Guest Restraint and Simulation Window Details

Details for each simulation set in Table 1 are as follows:

CB7-All8: attachment of the guest restraints and host conformational restraints was accomplished over 15 windows with spacing clustered near the lower values of λ_p,λ_c (7 windows less than λ_p,λ_c=0.3) with the exception of the B2 guest, which used 29 windows for testing purposes; host conformational restraints included 14 distance restraints spanning opposing nitrogen atoms with a final force constant of 6.0 kcal/mol-Å^2 and target distance of 12.3 Å; flatwell restraints to prevent dissociation of unrestrained guests were not used; the final guest distance restraint force constant was 10.0 kcal/mol-Å^2 for G8, G9, and MVN, and 5.0 kcal/mol-Å^2 for all others; the angle/torsion force constants were 100.0 kcal/mol-rad^2; the pulling phase consisted of varying the guest distance restraint from 6.0 Å to 24.0 Å for all guests except B11 which required pulling to 30.0 Å due to its greater size; the pulling phase was divided into increments of 0.25 Å for guests G8, G9, and MVN and increments of 0.40 Å for all others; the host conformational restraints were released with identical λ_c spacing as the attachment phase but without a guest in the simulation; a separate host release calculation was performed with a single Tris buffer molecule included in order to match experimental conditions for the MVN measurement.

CB7-B2$_{Temp}$: attachment was accomplished over 41 windows with uniform spacing of λ_p,λ_c; host conformational restraints included 14 distance restraints spanning opposing nitrogen atoms with a final force constant of 15.0 kcal/mol-Å^2 and target distance of 13.5 Å; flatwell restraints were not used; the final guest distance restraint force constant was 10.0 kcal/mol-Å^2 and the angle/torsion force constants were 100.0 kcal/mol-rad^2; the pulling phase consisted of 73 windows in which the guest distance restraint was varied from 6.0 Å to 24.0 Å in increments of 0.25 Å; the release phase for the host conformational restraints was identical to the attachment phase except that the guest was in the unbound position and its restraints were held constant.

CB7-B2$_{HMR}$: the restraint setup for all simulation phases were identical to those of CB7-B2$_{Temp}$.

βCD-Hex$_{Temp}$: the attachment phase was accomplished with 44 windows using uniform spacing of λ_p,λ_c with the exception of two additional windows at 0.0100 and 0.0375; the final guest restraint force constants were 10.0 kcal/mol-Å^2 on the distance restraint and 100.0 kcal/mol-rad^2 on the angle/torsion restraints; constant 10.0 kcal/ mol-Å^2 flatwell restraints were added to prevent complete dissociation of the host-guest complex which can occur on the 1 μs timescale of simulation windows with very low λ_p,λ_c values; host conformational restraints added during the attachment phases consisted of two torsion restraints per glucopyranoside monomer on the O5$_n$-C1$_n$-O1$_n$-C4$_{n+1}$, and C1$_n$-O1$_n$-C4$_{n+1}$-C5$_{n+1}$ atoms with respective target restraint values of 108.7° and -112.5° and a final force constant of 6.0 kcal/mol-rad^2; the pulling phase consisted of 73 windows in which the guest distance restraint was varied from 6.0 Å to 24.0

Å in increments of 0.25 Å; the host conformational restraint release phase was carried out without the guest present and used the same spacing as the attachment phase.

βCD-Hex$_{HMR}$: attachment phase simulations consisted of 15 windows with non-uniform spacing of λ_p,λ_c in which window density was concentrated at low values (8 windows less than λ_p,λ_c=0.1); host conformation restraints were identical to those in βCD-Hex$_{Temp;}$ the final guest restraint force constants were 5.0 kcal/mol-Å^2 on the distance restraint and 100.0 kcal/mol-rad^2 on the angle/torsion restraints, constant flatwell restraints were employed identically as those for βCD-Hex$_{Temp}$, the pulling phase guest distance restraint was varied from 6.0 Å to 24.0 Å in increments of 0.40 Å; the host conformational restraint release phase was identical to βCD-Hex$_{Temp}$.

βCD-Hex$_{Alt}$: these simulations were identical to the βCD-Hex$_{Temp}$ simulations except the atom identities involved in each restraint was changed in order to test whether the results depending on this choice.

K-Cl$_{Simple}$: a single distance restraint was attached over 53 independent windows with spacing density near low λ_p values (14 windows less than λ_p=0.025); the final distant restraint force constant was 10.0 kcal/mol-Å^2; a constant flatwell restraint was included to maintain the bound state; the pulling phase consisted of 65 windows moving between a target restraint distance of 2.65 Å and 18.65 Å with 0.25 Å spacing.

K-Cl$_{Temp}$: attachment of the guest restraints used identical window spacing as K-Cl$_{Simple}$ including the constant flatwell restraint except that the anchor particle scheme was used (Figure S2); the final force constant for the distance restraint was 10.0 kcal/mol-Å^2 and for the angle restraint was 100.0 kcal/mol-rad^2; the pulling phase was identical to that for K-Cl$_{Simple}$ except the distance restraint starts at 8.65 Å and ends at 24.65 Å due to the offset anchor particles.

Note that, in all simulation sets, the final window of the attachment phase is identical to the first window of the pulling phase. Likewise, the pulling phase and conformational restraint release phase share a common simulation window.

Equation Details

Here we provide additional details for deriving the force for the attachment and pulling steps. Refer to Equation 2 and its explanatory paragraph for context:

The "force" of attaching restraints is λ-dependent and can be found by taking the partial derivative of μ_{hg}° with respect to λ_p and λ_c.

$$\begin{aligned}\langle F\rangle_{\lambda_p,\lambda_c} &= \frac{\partial \mu_{hg}^{\circ}}{\partial \lambda_p} + \frac{\partial \mu_{hg}^{\circ}}{\partial \lambda_c} \\ &= \frac{\int \left[\sum_{n=1}^{N_p} k_n^p (x_n^p - x_{0,n}^p)^2\right] e^{-\beta\left[E(X)+\sum_{n=1}^{N_p}\lambda_p k_n^p (x_n^p - x_{0,n}^p)^2 + \sum_{n=1}^{N_c}\lambda_c k_n^c \left(x_n^c - x_{0,n}^c\right)^2\right]} dX}{\int e^{-\beta\left[E(X)+\sum_{n=1}^{N_p}\lambda_p k_n^p (x_n^p - x_{0,n}^p)^2 + \sum_{n=1}^{N_c}\lambda_c k_n^c \left(x_n^c - x_{0,n}^c\right)^2\right]} dX} \\ &+ \frac{\int \left[\sum_{n=1}^{N_c} k_n^c \left(x_n^c - x_{0,n}^c\right)^2\right] e^{-\beta\left[E(X)+\sum_{n=1}^{N_p}\lambda_p k_n^p (x_n^p - x_{0,n}^p)^2 + \sum_{n=1}^{N_c}\lambda_c k_n^c \left(x_n^c - x_{0,n}^c\right)^2\right]} dX}{\int e^{-\beta\left[E(X)+\sum_{n=1}^{N_p}\lambda_p k_n^p (x_n^p - x_{0,n}^p)^2 + \sum_{n=1}^{N_c}\lambda_c k_n^c \left(x_n^c - x_{0,n}^c\right)^2\right]} dX} \\ &= \sum_{n=1}^{N_p} k_n^p \left\langle \left(x_n^p - x_{0,n}^p\right)^2 \right\rangle_{\lambda_p} + \sum_{n=1}^{N_c} k_n^c \left\langle \left(x_n^c - x_{0,n}^c\right)^2 \right\rangle_{\lambda_c}\end{aligned} \tag{3}$$

The mean pulling force is the partial derivative of the chemical potential with respect to the varying parameter, $x_{0,1}^p$, used for pulling:

$$\begin{aligned}\langle F\rangle_{x_{0,1}^p} &= \frac{\partial \mu_{hg}^{\circ}}{\partial x_{0,1}^p} \\ &= -\frac{\int \left[2k_1^p \left(x_1^p - x_{0,1}^p\right)\right] e^{-\beta\left[E(X)+\sum_{n=1}^{N_p}\lambda_p k_n^p (x_n^p - x_{0,n}^p)^2 + \sum_{n=1}^{N_c}\lambda_c k_n^c \left(x_n^c - x_{0,n}^c\right)^2\right]} dX}{\int e^{-\beta\left[E(X)+\sum_{n=1}^{N_p}\lambda_p k_n^p (x_n^p - x_{0,n}^p)^2 + \sum_{n=1}^{N_c}\lambda_c k_n^c \left(x_n^c - x_{0,n}^c\right)^2\right]} dX} \\ &= -2k_1^p \left\langle x_1^p - x_{0,1}^p \right\rangle\end{aligned} \tag{5}$$

Table S1. Thermodynamic values computed for the CB7 simulation sets.

Simulation Set (Guest), Temperature, Calculated Value	Number of Windows	Total Simulation Time (ns)	TI/block (kcal/mol)	MBAR/StIn (kcal/mol)
CB7-All8 (A1), 300 K, ΔG_{bind}	90	4720	-23.74 ±0.29	-23.96 ±0.48
CB7-All8 (A1), 300 K, ΔH_{bind} Dir	2	2000	-24.89 ±0.43	-24.89 ±0.36
CB7-All8 (A2), 300 K, ΔG_{bind}	104	4860	-27.41 ±0.27	-27.45 ±0.17
CB7-All8 (A2), 300 K, ΔH_{bind} Dir	2	2000	-22.64 ±0.60	-22.64 ±0.36
CB7-All8 (B2), 300 K, ΔG_{bind}	90	5275	-21.25 ±0.22	-21.22 ±0.26
CB7-All8 (B2), 300 K, ΔH_{bind} Dir	2	2000	-21.59 ±0.41	-21.59 ±0.36
CB7-All8 (B5), 300 K, ΔG_{bind}	90	5260	-27.12 ±0.36	-27.25 ±0.59
CB7-All8 (B5), 300 K, ΔH_{bind} Dir	2	2000	-18.27 ±0.48	-18.27 ±0.36
CB7-All8 (B11), 300 K, ΔG_{bind}	105	8825	-30.41 ±0.81	-30.26 ±0.72
CB7-All8 (B11), 300 K, ΔH_{bind} Dir	2	2000	-17.71 ±0.48	-17.71 ±0.39
CB7-All8 (G8), 300 K, ΔG_{bind}	117	5855	-13.89 ±0.29	-13.93 ±0.28
CB7-All8 (G8), 300 K, ΔH_{bind} Dir	2	2000	-6.26 ±0.48	-6.26 ±0.36
CB7-All8 (G9), 300 K, ΔG_{bind}	117	6385	-18.49 ±0.59	-18.64 ±1.13
CB7-All8 (G9), 300 K, ΔH_{bind} Dir	2	2000	-11.68 ±0.54	-11.68 ±0.36
CB7-All8 (MVN), 300 K, ΔG_{bind}	117	3385	-11.07 ±0.68	-10.68 ±0.65
CB7-All8 (MVN), 300 K, ΔH_{bind} Dir	2	2000	-2.34 ±0.53	-2.34 ±0.36
CB7-B2$_{Temp}$, 282 K, ΔG_{bind}	153	15905	-21.33 ±0.12	-21.37 ±0.07
CB7-B2$_{Temp}$, 288 K, ΔG_{bind}	153	15435	-21.41 ±0.12	-21.46 ±0.07
CB7-B2$_{Temp}$, 294 K, ΔG_{bind}	153	15420	-21.54 ±0.12	-21.58 ±0.07
CB7-B2$_{Temp}$, 300 K, ΔG_{bind}	153	18100	-21.32 ±0.13	-21.36 ±0.07
CB7-B2$_{Temp}$, 306 K, ΔG_{bind}	153	15300	-21.45 ±0.12	-21.52 ±0.07
CB7-B2$_{Temp}$, 312 K, ΔG_{bind}	153	15500	-21.50 ±0.11	-21.54 ±0.07
CB7-B2$_{Temp}$, 318 K, ΔG_{bind}	153	15430	-21.43 ±0.11	-21.50 ±0.07
CB7-B2$_{Temp}$, 300 K, ΔH_{bind} VH	1071	111090	-20.78 ±1.09	-20.66 ±0.67
CB7-B2$_{Temp}$, 300 K, ΔH_{bind} Dir	2	3000	-21.65 ±0.47	-21.65 ±0.28
CB7-B2$_{HMR}$, 300 K, ΔG_{bind}	153	13094	-21.27 ±0.41	-21.33 ±0.12
CB7-B2$_{HMR}$, 300 K, ΔH_{bind} Dir	2	4000	-21.78 ±0.44	-21.78 ±0.31

Notes: “Dir” and “VH” indicate direct and van’t Hoff binding enthalpy calculations, respectively. Data was collected every 0.5 ps for CB7-All8, every 1 ps for CB7-B2$_{Temp}$, and every 2 ps for CB7-B2$_{HMR}$. The conformational restraint release phase was performed separately from attach and pull phases for the CB7-All8 simulation set, but here its simulation time was included in the total for each ΔG value. See Table 1 for the aggregate simulation time collected for the entire simulation set. Uncertainty is given in 95% CI.

Table S2. Thermodynamic values calculated for the βCD-Hex simulation sets.

Simulation Set, Temperature, Quantity Calculated	Number of Windows	Total Simulation Time (ns)	TI/block (kcal/mol)	MBAR/StIn (kcal/mol)
βCD-Hex$_{Temp}$, 280 K, $\Delta G_{primary}$	160	28580	-2.66 ±0.23	-2.60 ±0.11
βCD-Hex$_{Temp}$, 290 K, $\Delta G_{primary}$	160	24844	-2.52 ±0.19	-2.58 ±0.10
βCD-Hex$_{Temp}$, 300 K, $\Delta G_{primary}$	161	20180	-2.64 ±0.20	-2.66 ±0.10
βCD-Hex$_{Temp}$, 310 K, $\Delta G_{primary}$	160	18000	-2.54 ±0.25	-2.71 ±0.11
βCD-Hex$_{Temp}$, 320 K, $\Delta G_{primary}$	160	14799	-2.79 ±0.18	-2.78 ±0.11
βCD-Hex$_{Temp}$, 280 K, $\Delta G_{secondary}$	160	27470	-3.56 ±0.23	-3.50 ±0.11
βCD-Hex$_{Temp}$, 290 K, $\Delta G_{secondary}$	160	24271	-3.76 ±0.19	-3.78 ±0.10
βCD-Hex$_{Temp}$, 300 K, $\Delta G_{secondary}$	161	20109	-3.78 ±0.20	-3.77 ±0.10
βCD-Hex$_{Temp}$, 310 K, $\Delta G_{secondary}$	160	17856	-3.93 ±0.22	-4.01 ±0.11
βCD-Hex$_{Temp}$, 320 K, $\Delta G_{secondary}$	160	15638	-4.00 ±0.19	-4.00 ±0.11
βCD-Hex$_{Temp}$, 280 K, ΔG_{bind}	276	45710	-3.66 ±0.19	-3.60 ±0.09
βCD-Hex$_{Temp}$, 290 K, ΔG_{bind}	276	39429	-3.83 ±0.17	-3.84 ±0.09
βCD-Hex$_{Temp}$, 300 K, ΔG_{bind}	278	33849	-3.86 ±0.17	-3.86 ±0.09
βCD-Hex$_{Temp}$, 310 K, ΔG_{bind}	276	29620	-4.00 ±0.20	-4.08 ±0.10
βCD-Hex$_{Temp}$, 320 K, ΔG_{bind}	276	25928	-4.09 ±0.16	-4.08 ±0.09
βCD-Hex$_{Temp}$, 300 K, ΔH_{bind} VH	1382	174536	-0.81 ±1.72	-0.38 ±0.89
βCD-Hex$_{Temp}$, 300 K, $\Delta H_{primary}$ Dir	2	2000	-1.58 ±0.56	-1.58 ±0.39
βCD-Hex$_{Temp}$, 300 K, $\Delta H_{secondary}$ Dir	2	2000	-1.03 ±0.52	-1.04 ±0.38
βCD-Hex$_{Temp}$, 300 K, ΔH_{bind} Dir	278	33849	-1.13 ±0.66	-1.11 ±0.41
βCD-Hex$_{HMR}$, 300 K, $\Delta G_{primary}$	76	12715	-2.60 ±0.22	-2.54 ±0.10
βCD-Hex$_{HMR}$, 300 K, $\Delta G_{secondary}$	76	12755	-3.91 ±0.23	-3.86 ±0.10
βCD-Hex$_{HMR}$, 300 K, ΔG_{bind}	137	16955	-3.98 ±0.21	-3.92 ±0.09
βCD-Hex$_{HMR}$, 300 K, $\Delta H_{primary}$ Dir	2	2000	-1.39 ±0.60	-1.39 ±0.43
βCD-Hex$_{HMR}$, 300 K, $\Delta H_{secondary}$ Dir	2	2000	-0.14 ±0.64	-0.14 ±0.41
βCD-Hex$_{HMR}$, 300 K, ΔH_{bind} Dir	137	16955	-0.27 ±0.64	-0.26 ±0.39
βCD-Hex$_{Alt}$, 300 K, $\Delta G_{primary}$	159	13958	-2.60 ±0.39	-2.58 ±0.18
βCD-Hex$_{Alt}$, 300 K, $\Delta H_{primary}$ Dir	2	2000	-1.37 ±0.67	-1.37 ±0.38

Notes: "Dir" and "VH" indicate direct and van't Hoff binding enthalpy calculations, respectively. Data collected every 1 ps except for βCD-Hex$_{HMR}$ which collected every 0.5 ps. The conformational restraint release phase was performed separately from attach and pull phases, but here its simulation time was included in the total for each $\Delta G_{primary}$ and $\Delta G_{secondary}$ value listed. It was only included once for the ΔG_{bind} values. See Table 1 for the aggregate simulation time collected for the entire simulation set. Uncertainty is given in 95% CI.

Table S3. Thermodynamic values calculated for the K-Cl ion pair system.

Simulation Set, Temperature, Quantity Calculated	Number of Windows	Total Simulation Time (ns)	TI/block (kcal/mol)	MBAR/StIn (kcal/mol)
$K\text{-}Cl_{Simple}$, 300 K, ΔG_{bind}	117	4000	-1.92 ±0.14	-1.86 ±0.10
$K\text{-}Cl_{Simple}$, 300 K, ΔH_{bind} Dir	2	2000	3.45 ±0.39	3.45 ±0.35
$K\text{-}Cl_{Temp}$, 280 K, ΔG_{bind}	117	13989	-1.65 ±0.06	-1.63 ±0.04
$K\text{-}Cl_{Temp}$, 290 K, ΔG_{bind}	117	13730	-1.74 ±0.06	-1.75 ±0.04
$K\text{-}Cl_{Temp}$, 300 K, ΔG_{bind}	117	15143	-1.94 ±0.06	-1.94 ±0.04
$K\text{-}Cl_{Temp}$, 310 K, ΔG_{bind}	117	13050	-2.15 ±0.06	-2.15 ±0.05
$K\text{-}Cl_{Temp}$, 320 K, ΔG_{bind}	117	13651	-2.32 ±0.06	-2.34 ±0.05
$K\text{-}Cl_{Temp}$, 300 K, ΔH_{bind} VH	585	69563	3.35 ±0.55	3.58 ±0.42
$K\text{-}Cl_{Temp}$, 300 K, ΔH_{bind} Dir	2	2312	3.68 ±0.28	3.68 ±0.23

Notes: “Dir” and “VH” indicate direct and van’t Hoff binding enthalpy calculations, respectively. Data collected every 1 ps. MBAR was limited to 100000 statistically independent frames per window due to memory constraints. Uncertainty is given in 95% CI.

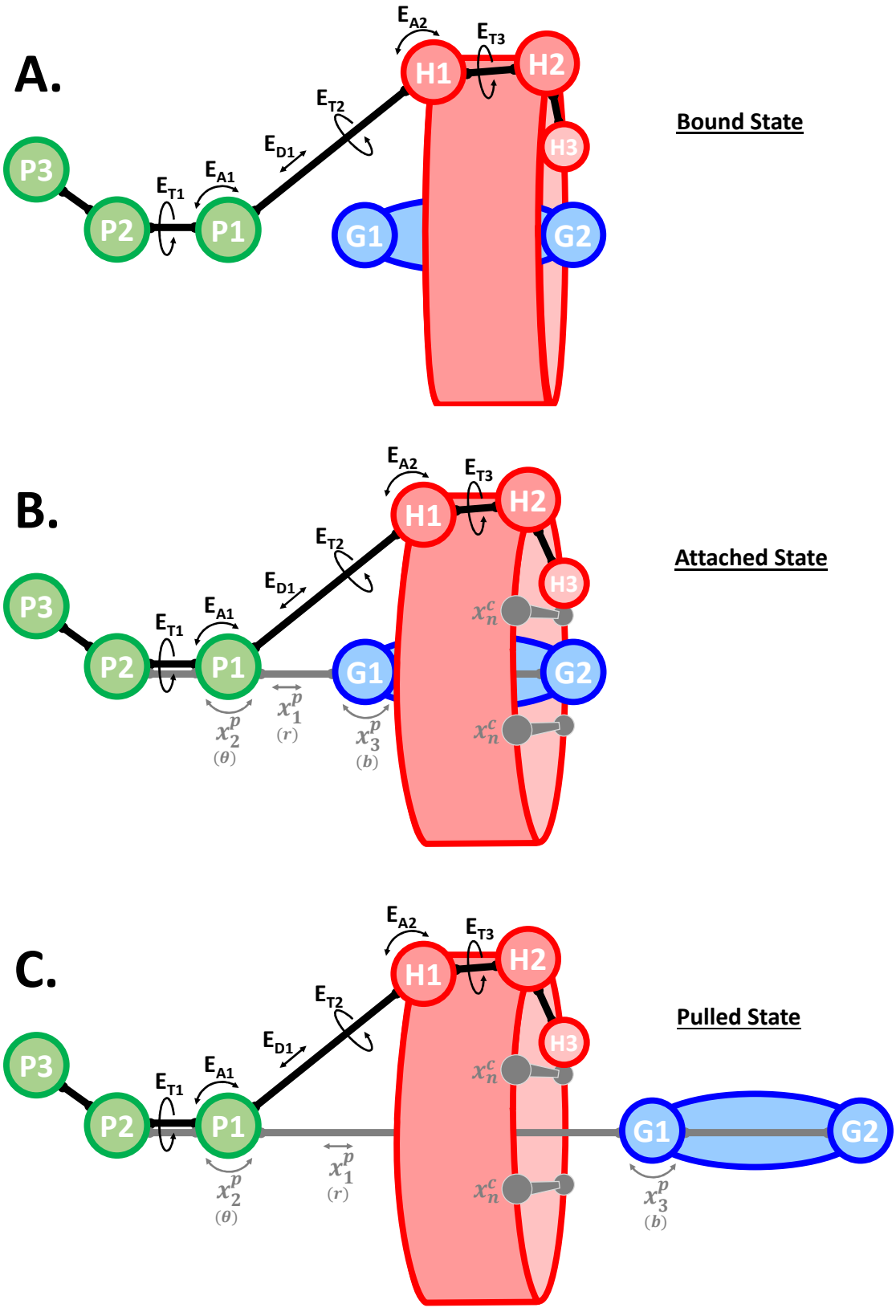

Figure S1. (continued on next page)

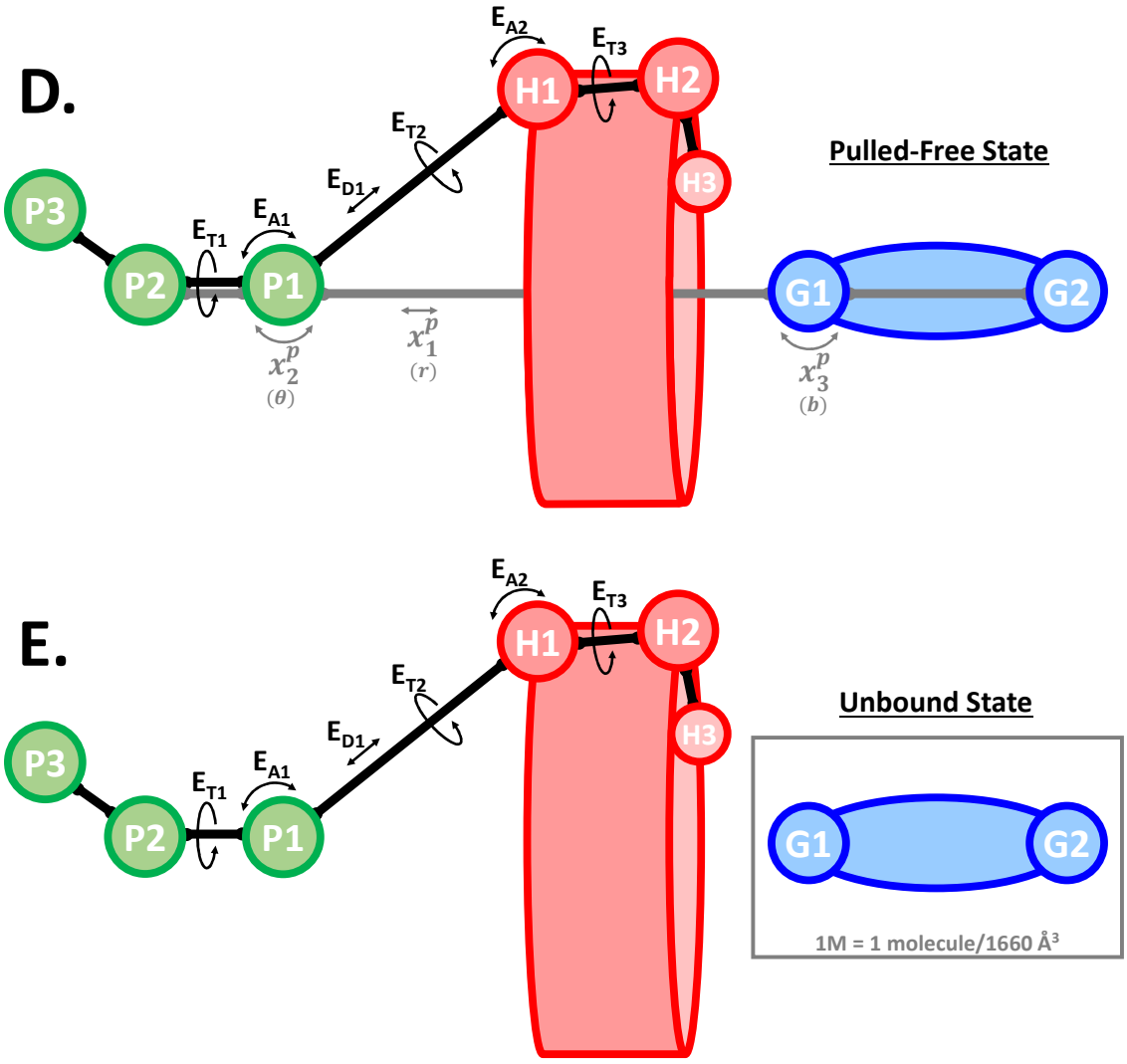

Figure S1. (continued) Restraint scheme demonstrating the use of anchor particles for attach-pull-release (APR) free energy calculations. P1-3 are anchor particles, H1-3 are host atoms, and G1-2 are guest atoms. The E_{D1}, E_{A1-2}, and E_{T1-3} labels indicate distance, angle, and torsion restraints, respectively, which modify the host translational and rotational degrees of freedom and are included implicitly in the potential energy function, $E(X)$, as described in the main text. These restraints are held constant throughout all simulation windows and do not perturb the host's conformational degrees of freedom. Indicated in gray with labels x_1^p, x_2^p, x_3^p, and x_n^c are restraints which are attached over a series of simulation windows and are subsequently used to pull the guest out of the host cavity. In this example, x_1^p is a distance restraint, x_2^p and x_3^p are angle restraints, and x_n^c represents host conformational restraints (of any harmonic form). In parenthesis, the corresponding spherical coordinate or Euler angle is indicated for each translational/rotational pose restraint, as defined in the main text.

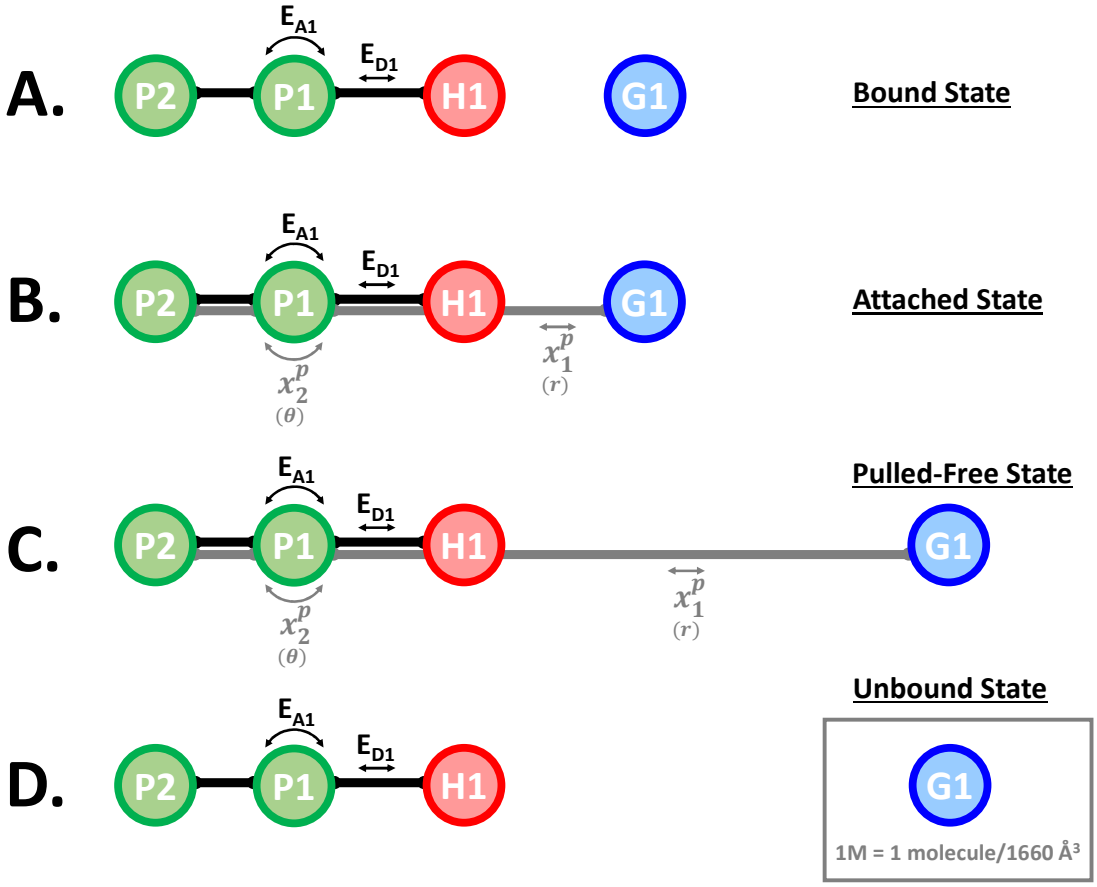

Figure S2. Restraint scheme demonstrating the use of anchor particles for attach-pull-release (APR) free energy calculations on an ion pair. P1-2 are anchor particles, H1 is the "host" ion, and G1 is the "guest" ion. The E_{D1} and E_{A1} labels indicate distance and angle restraints, respectively, which restraint the "host" ion translational and rotational degrees of freedom and are included implicitly in the potential energy function, $E(X)$, as described in the main text. These restraints are held constant throughout all simulation windows. The x_1^p and x_2^p, labels indicate a distance and angle restraint which are attached to the "guest" ion and used to pull the ions apart. In parenthesis, the corresponding spherical coordinate or Euler angle is indicated for each translational/rotational pose restraint, as defined in the main text. Note that there is no "Pulled State" since there are no conformational restraints to release.

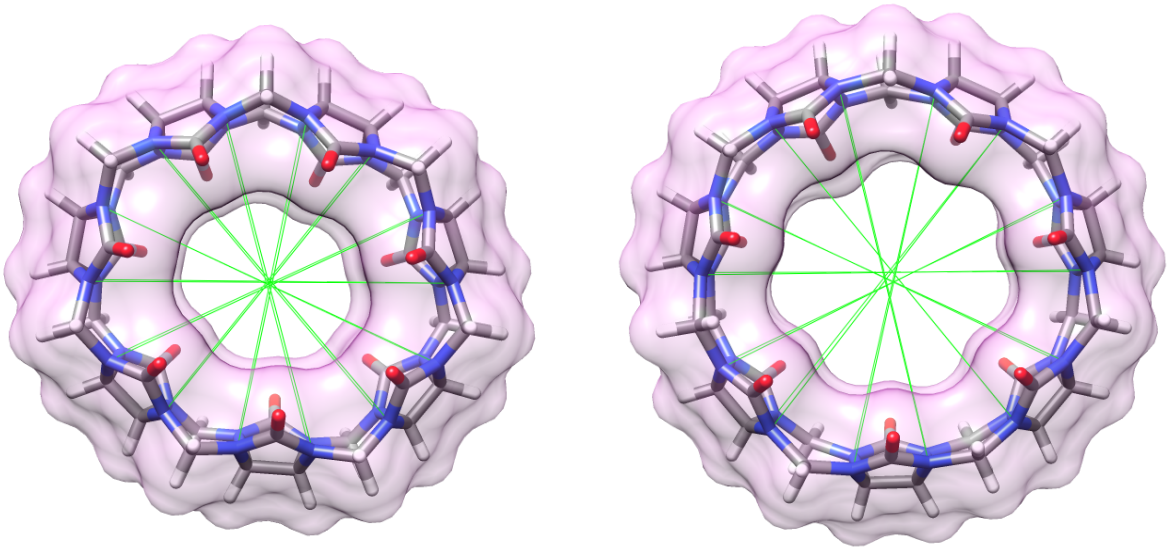

Figure S3. Effect of conformational restraints on CB7 structure. Conformational distance restraints are represented by green lines. At left is the CB7 molecule with the restraints turned off. At right is with the restraints turned on.

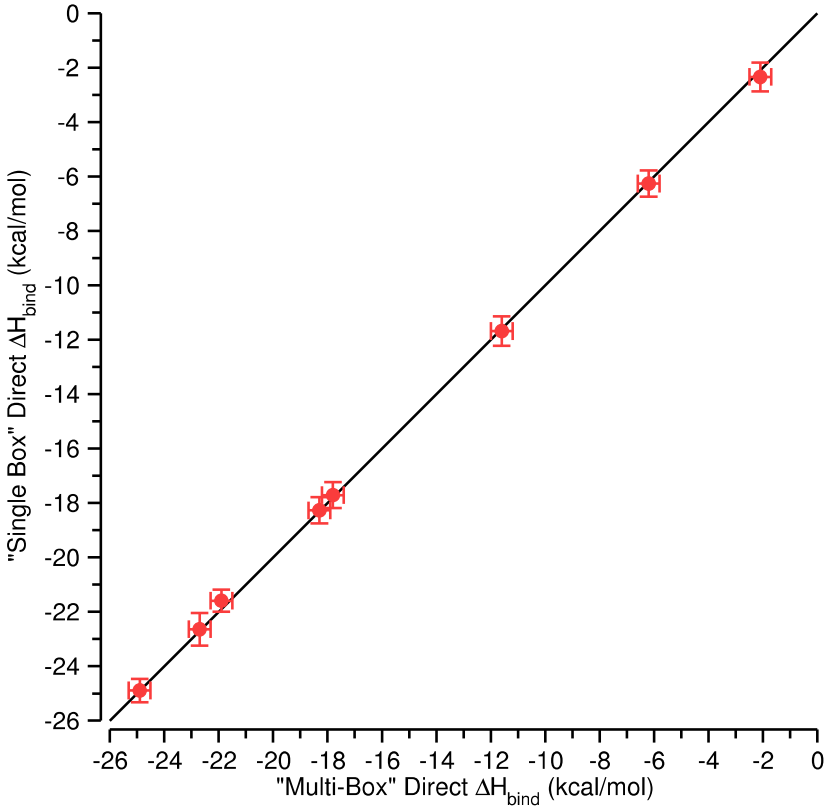

Figure S4. Correlation between the binding enthalpy computed using the "multi-box" approach[1] and the "one-box" approach used in this work. The RMSD between the two data sets is 0.148 kcal/mol and the R value is 0.99992.

(1) Fenley, A. T.; Henriksen, N. M.; Muddana, H. S.; Gilson, M. K. Bridging Calorimetry and Simulation through Precise Calculations of Cucurbituril–Guest Binding Enthalpies. *J. Chem. Theory Comput.* **2014**, *10* (9), 4069–4078.

3.25

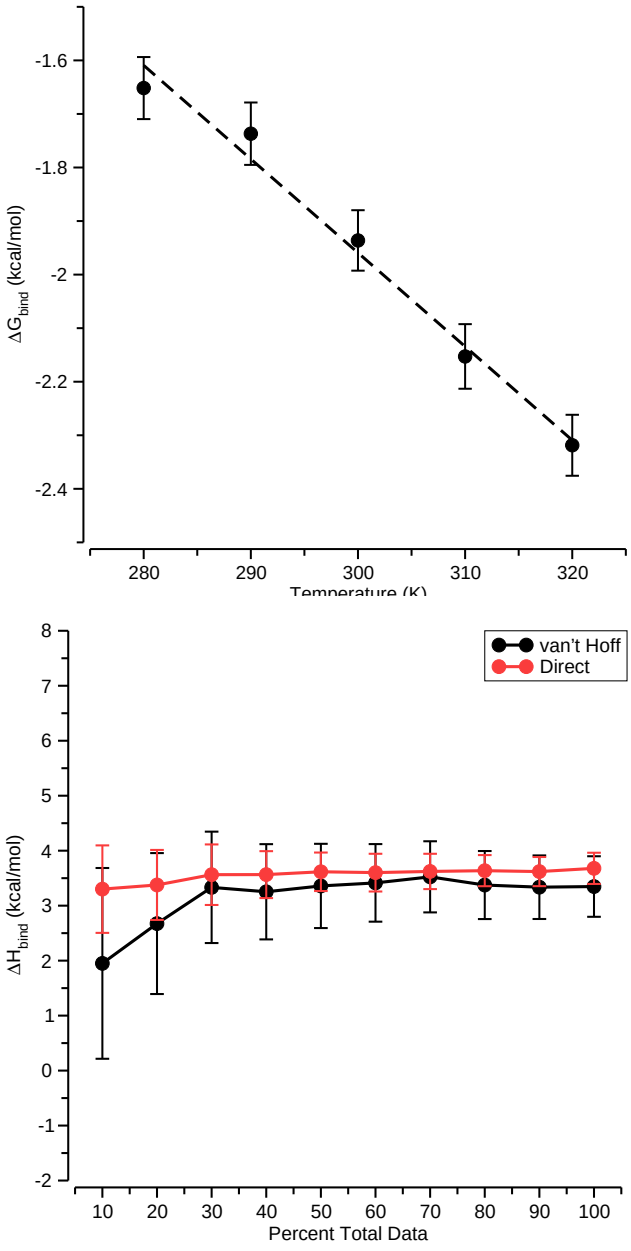

Figure S5. Demonstration of the temperature dependence of the binding free energy (top) and the convergence of the van't Hoff and direct binding enthalpy calculations at 300 K (bottom) for the K-Cl_{Temp} simulation set.

Figure S6. Python Code to generate artificially correlated data. The code is intended to generate correlated data with blocking curve shapes that mimic those observed in real host-guest data (see Figure 8, bottom). This is achieved by mixing large-variance-short-correlation processes with small-variance-long-correlation processes.

```
import numpy as np # numerical array library

Ne = 50000  ### Number of equilibration points
Np = 500000 ### Number of production points
Nf = 500    ### Number of files (runs)

### Correlated Decay Processes (rho= memory, amp= amplitude)
rho = [0.05, 0.85, 0.85, 0.85, 0.85, 0.85, 0.85, 0.85, 0.85, 0.85, 0.85, 0.85]
amp = 61.0

### Correlated "Jumper" Value
jamp = 5.0 ### Jumper Amplitude
jint = 10000 ### Jumper target interval
rjv = np.random.normal(0.0,jamp) ### Random Jumper value
rji = np.random.randint(1,jint) ### Random Jumper interval

for f in range(Nf): ### For each file ....
  datfile = open('series-'+str(f)+'.dat', 'w')
  ov = [0]*len(rho)   ### Old Value
  for j in range (len(rho)):
    ov[j] = np.random.normal(0.0,amp) ### Initialize Correlated decay values
  nv = [0]*len(rho)   ### New Value
  for i in range(Ne+Np): ### For each "simulation" point ....
    sv = 0.0  ### Sum value
    for j in range (len(rho)): ### For each decay process ...
      nv[j] = (rho[j]*ov[j] + (1-rho[j])*np.random.normal(0.0,amp))
      sv += nv[j]
      ov[j] = nv[j]
    if i % rji == 0:  ### Jump the "Jumper"?
      rjv = np.random.normal(0.0,jamp)
      rji = i + np.random.randint(1,jint)
    if i >= Ne:  ### Write the value if we have finished equilibration
      sv += rjv
      datfile.write("%12.7f\n" % (sv) )
  datfile.close()
```

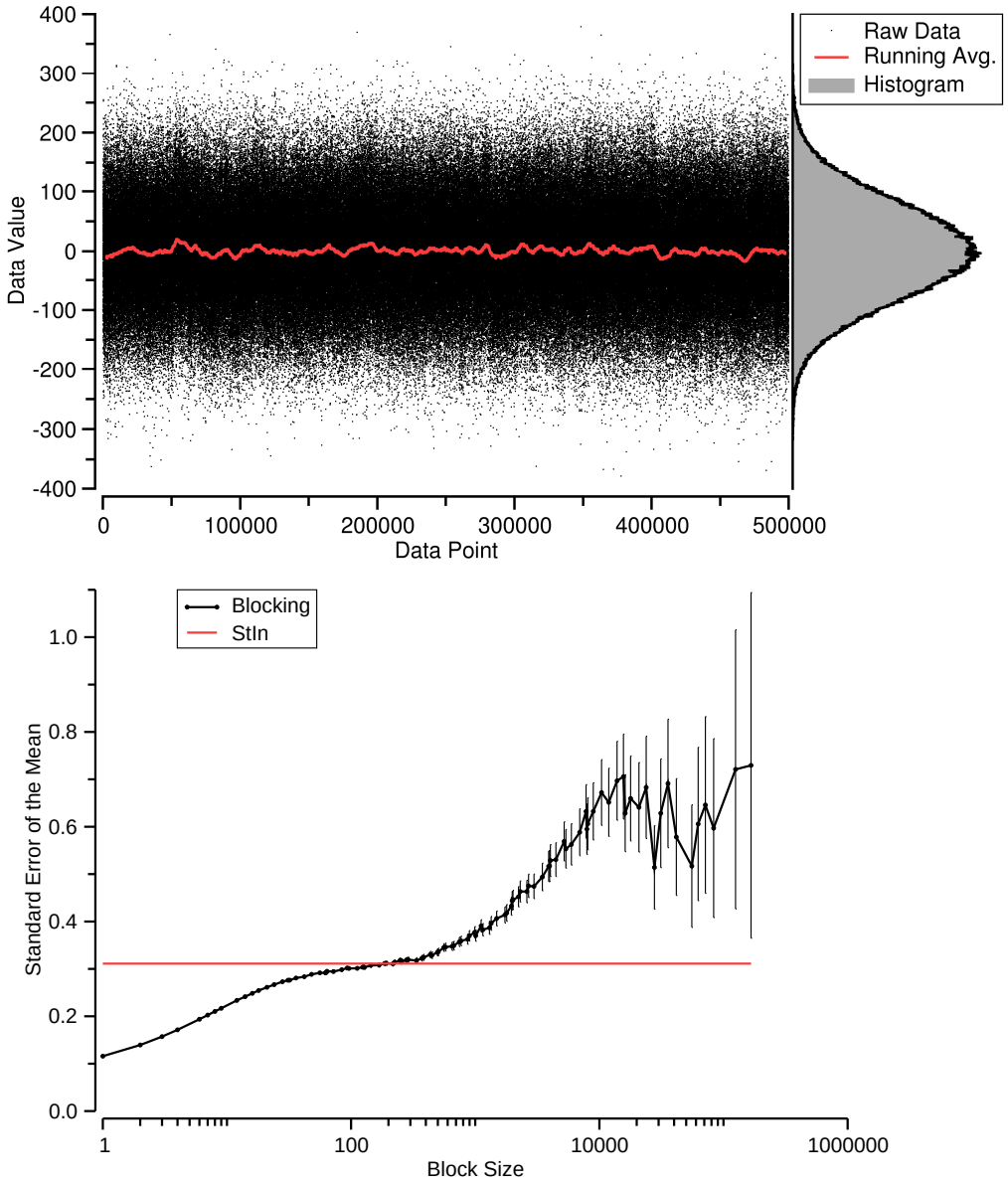

Figure S7. Example of an artificial dataset generated by the code in Figure S6. (Top) Plot of the raw data values (black dots) versus data point position (i.e., "time"). A running average over 5000 points (red) and a histogram of the data (grey) is provided. (Bottom) A blocking curve (black) and StIn SEM estimate (red line) for the dataset in the top panel. Compare with blocking curves for real host-guest simulations in Figure 8, bottom.